Title

The Aftermath of Surviving Acute Radiation Hematopoietic Syndrome and its Mitigation

Journal

Radiation Research, 191(4)

ISSN

0033-7587

Authors

Micewicz, Ewa D

Iwamoto, Keisuke S

Ratikan, Josephine A

et al.

Publication Date

2019-04-01

DOI

10.1667/rr15231.1

Peer reviewed

RADIATION RESEARCH **191**, 323–334 (2019)
0033-7587/19 $15.00

DOI: 10.1667/RR15231.1

The Aftermath of Surviving Acute Radiation Hematopoietic Syndrome and its Mitigation

Ewa D. Micewicz,[a] Keisuke S. Iwamoto,[a] Josephine A. Ratikan,[a] Christine Nguyen,[a] Michael W. Xie,[a] Genhong Cheng,[b] Gayle M. Boxx,[b] Elisa Deriu,[b] Robert D. Damoiseaux,[g] Julian P. Whitelegge,[h] Piotr P. Ruchala,[h] Rozeta Avetisyan,[c] Michael E. Jung,[d] Greg Lawson,[e] Elizabeta Nemeth,[f] Tomas Ganz,[f] James W. Sayre,[i] William H. McBride[a] and Dörthe Schaue[a,1]

Departments of [a] Radiation Oncology, [b] Microbiology, Immunology and Molecular Genetics, [c] Anesthesiology, [d] Chemistry and Biochemistry, [e] Laboratory Animal Medicine, [f] Medicine, [g] Molecular Screening Shared Resource, [h] Pasarow Mass Spectrometry Laboratory and [i] School of Public Health, Biostatistics and Radiology, University of California at Los Angeles, Los Angeles, California

Micewicz, E. D., Iwamoto, K. S., Ratikan, J. A., Nguyen, C., Xie, M. W., Cheng, G., Boxx, G. M., Deriu, E., Damoiseaux, R. D., Whitelegge, J. P., Ruchala, P. P., Avetisyan, R., Jung, M. E., Lawson, G., Nemeth, E., Ganz, T., Sayre, J. W., McBride, W. H. and Schaue, D. The Aftermath of Surviving Acute Radiation Hematopoietic Syndrome and its Mitigation. *Radiat. Res.* 191, 323–334 (2019).

Intensive research is underway to find new agents that can successfully mitigate the acute effects of radiation exposure. This is primarily in response to potential counterthreats of radiological terrorism and nuclear accidents but there is some hope that they might also be of value for cancer patients treated with radiation therapy. Research into mitigation countermeasures typically employs classic animal models of acute radiation syndromes (ARS) that develop after whole-body irradiation (WBI). While agents are available that successfully mitigate ARS when given after radiation exposure, their success raises questions as to whether they simply delay lethality or unmask potentially lethal radiation pathologies that may appear later in time. Life shortening is a well-known consequence of WBI in humans and experimental animals, but it is not often examined in a mitigation setting and its causes, other than cancer, are not well-defined. This is in large part because delayed effects of acute radiation exposure (DEARE) do not follow the strict time–dose phenomena associated with ARS and present as a diverse range of symptoms and pathologies with low mortality rates that can be evaluated only with the use of large cohorts of subjects, as in this study. Here, we describe chronically increased mortality rates up to 660 days in large numbers of mice given $LD_{70/30}$ doses of WBI. Systemic myeloid cell activation after WBI persists in some mice and is associated with late immunophenotypic changes and hematopoietic imbalance. Histopathological changes are largely of a chronic inflammatory nature and variable incidence, as are the clinical symptoms, including late diarrhea that correlates temporally with changes in the content of the microbiome. We also describe the acute and long-term consequences of mitigating hematopoietic ARS (H-ARS) lethality after $LD_{70/30}$ doses of WBI in multiple cohorts of mice treated uniformly with radiation mitigators that have a common 4-nitrophenylsulfonamide (NPS) pharmacophore. Effective NPS mitigators dramatically decrease ARS mortality. There is slightly increased subacute mortality, but the rate of late mortalities is slowed, allowing some mice to live a normal life span, which is not the case for WBI controls. The study has broad relevance to radiation late effects and their potential mitigation and epitomizes the complex interaction between radiation-damaged tissues and immune homeostasis.

INTRODUCTION

Rarely has a threat of exposure to an agent captivated and terrified humans like that of ionizing radiation. Considering the current political climate, it is not surprising that the fear of nuclear terrorism has renewed efforts to develop countermeasures of radiation mortality and morbidity, with some success (*1–7*). At the same time, enhanced survivorship in patients receiving clinical radiation therapy for cancer has increased the prevalence of late morbidities, and it is reasonable to suggest that some of these agents might be repurposed for such conditions.

Since the 1950s, whole-body irradiation (WBI) has been known to precipitate late morbidity and mortality with consequential ''life shortening,'' which is a complex phenomenon attributed to both non-cancerous and cancerous conditions (*8–11*). The former is at least as important as the latter (*12*), but much more difficult to define. This is because the symptoms associated with the delayed effects of acute radiation exposure (DEARE), although dose-related,

Editor's note. The online version of this article (DOI: 10.1667/RR15231.1) contains supplementary information that is available to all authorized users.

[1] Address for correspondence: Department of Radiation Oncology, UCLA David Geffen School of Medicine, B3-109 CHS, 10833 Le Conte Avenue, Los Angeles, CA 90095-1714; email: dschaue@mednet.ucla.edu.

do not follow the tight dose–time relationships that characterize acute radiation syndromes (ARS). For ARS, mortality increases rapidly from 0 to 100% within narrow dose/time limits characteristic for each tissue-related syndrome (*13, 14*), with age (*15, 16*), genetic background (*13, 17*), and microbial status (18) as important variables. For example, studies with hematopoietic ARS (H-ARS) as an end point typically use WBI doses designed to be lethal for 70% of mice within a time window of 10 to 30 days ($LD_{70/30}$); mitigators are typically administered at least 1 day postirradiation.

DEARE, in contrast, present as a diverse spectrum of symptoms and histopathological changes in mice and man that occur over a long time period (*12, 16, 19*). So, human A-bomb survivors have been reported to develop dose-related, significant rises in thyroid and liver disease, cataracts, glaucoma, hypertension and myocardial infarction (*20, 21*), as well as having persistently altered immune and inflammatory status (*22–25*). Survivors of the Tokai-mura criticality accident succumbed to a mixture of chronic hematological and late-onset non-hematological complications (*26, 27*), while exposure of workers at the Mayak facility to waterborne uranium fission products developed a variety of chronic diseases, including lung fibrosis (*28*). Nonhuman primates have been found to develop late onset type 2 diabetes and cardiac disease after WBI (*29, 30*).

Currently, it is unclear whether mitigation of H-ARS alters DEARE incidence. In theory, mortality and morbidity may be simply delayed by ARS mitigation, with or without the appearance of novel symptoms. On the other hand, if mitigation can be equated with a lowering of radiation dose, DEARE might be lessened. It should be noted that if mitigators change the biological end point, dose modifying factors cannot be used for efficacy comparisons. Also, agents that protect against ARS do not necessarily prevent life shortening (*31*) and even bone marrow transplantation appears to do little to prevent DEARE in mice (*12, 19*) or humans, as survivors of childhood cancer treated with WBI along with bone marrow transplantation have a high, but variable, incidence of radiation pneumonitis, veno-occlusive disease, renal hypertension, cardiac damage, neurocognitive abnormalities, cataracts, endocrine dysfunction and hormonal deficits (*32*). A conventional theory for ARS is that irradiated tissues fail progressively, with the time to failure being dependent on tissue turnover. This does little to explain the relentless progression of DEARE over time, although their strong dose-rate dependency is consistent with damage to tissues with slow turnover (*19*).

The complexity and diversity inherent in DEARE inevitably dictates a necessity for large cohorts of subjects. In the course of our high-throughput screening of large chemical libraries for radiation mitigators, we discovered efficacy associated with a group of chemicals that have a 4-nitrophenylsulfonamide (NPS) pharmacophore in common (*33*). This allowed us to use, as a platform for examining DEARE, data from more than 600 mice largely of one strain, one gender, one microbiome, one WBI dose ($LD_{70/30}$), and one type of drug and route of administration over a 3-year period, with findings from other conditions added for broader applicability. Our findings are consistent with previously published studies of late effects of WBI in mice and man variably described as premature aging (*18, 34, 35*) or increased frailty (*36*). Most notably, we describe the variable occurrence of a persistent myeloid shift in WBI mice that was associated with imbalance in the immunohematopoietic system and that appears to have multiple long-term consequences. A role for the microbiome in late diarrhea is also suggested, which may have broader relevance. The findings support the contention that chronic inflammatory reactions are the thread that links early damage to the various manifestations of DEARE. The fact that multiple organs are involved supports our argument that DEARE has similarities to multiple organ disease (*37*). In this study, radiation-induced cancer incidence was low and, importantly, acute mitigator treatment allowed approximately one half of the animals to live a normal life span, compared to no animals without mitigation.

MATERIALS AND METHODS

Animals and Irradiation

Gnotobiotic, defined-flora, male C3Hf/Sed//Kam or C57Bl/6 mice were used to minimize the influence of different microbiomes on outcomes. They were bred in our AAALAC-accredited Radiation Oncology facility and entered into experiments at approximately 28 g body weight (with 1 SD $<$ 1 g; 9–12 weeks of age). Nonanesthetized mice were whole-body irradiated using an AEC Gammacell® 40 cesium source (Cs-137) at a dose rate of approximately 60 cGy/min. C3H/Sed mice received 7.725 Gy and C57BL/6 mice 8.509 Gy, which are institutional $LD_{70/30}$ estimates derived from prior probit analyses of H-ARS mortality. In reality, the average group survival for diluent-treated WBI C3H male mice from 50 different experiments averaged 26.5% $\pm$ 3.74 [1 standard error of the mean (SEM)] and both male and female C3H and C57BL/6 mice were similarly close to the expected 30%. For dosimetry, a Capintec ionization chamber calibrated to NIST standards was used, with Gafchromic™ EBT2 film (International Specialty Products, Wayne, NJ), to confirm that dose and field uniformity were within 5%. NIH guidelines and IACUC-approved protocols with defined criteria for premature euthanasia were closely followed. Animals were observed daily throughout the course of experiments, and at least twice a day during the peak period of H-ARS lethality (days 10–24).

Mitigation

The 4-nitrophenyl sulfonamide (NPS) or nitrophenylpiperazine (NPSP) compounds (Supplementary Fig. S1; http://dx.doi.org/10.1667/RR15231.1.S1) have been described elsewhere (*33*) and the reader is referred to this publication for a detailed background. In brief, the drugs came from a high-throughput screen for drugs able to mitigate radiation-induced lymphocytic apoptosis *in vitro* and H-ARS *in vivo*. They were purchased from ChemBridge™ Corp. (San Diego, CA) or synthesized in-house with purity and stability confirmed by nuclear magnetic resonance (NMR). All, including no drug controls, were resuspended in the same diluent (1% Cremophor) to minimize differences in solubility. We have shown independently that the diluent does not alter survival after WBI. Doses of drugs between 1 and 75 mg/kg, or diluent, were injected subcutaneously (s.c.) daily for

5 days starting at day +1 after WBI. A minority of mice were administered these drugs (or the diluent) either p.o. or with single s.c. doses. Since the findings are literally indistinguishable from those obtained by the s.c. injections, the data are included in the final analysis.

Echocardiography

Transthoracic echocardiograms were performed at monthly intervals, starting at 1 month, up to 1 year on individually marked mice that survived $LD_{70/30}$ WBI doses alongside age-matched nonirradiated controls. A Vevo 770 ultrasound system (VisualSonics Inc., Toronto, Canada) was used in the UCLA physiology core facility and operated by a single operator blind to the treatment. Inhaled isoflurane (induction 1.25% and maintenance 1%) maintains adequate sedation at a heart rate above 450 beats per min. A parasternal long-axis B-mode image was obtained. Fine adjustments were made to position the long axis of the left ventricular (LV) perpendicular to the ultrasound beam and to identify the maximal LV long- and short-axis. A 90° rotation at the papillary muscle level obtains a parasternal short-axis view of the LV. An M-mode image was captured to document LV dimensions and a semi-apical long-axis view of the LV. Pulse wave Doppler measurements data were used to determine LV ejection time, mitral flow E and A wave velocities, and quantitative measures obtained using the Vevo 770 cardiac analysis package.

Blood and Tissue Analysis

Blood was drawn from the retroorbital plexus in lightly anesthetized (isoflurane; Novaplus® Pharmaceuticals, Irving, TX) anesthetized mice using heparinized capillaries (Fisher Scientific™, Pittsburg, PA) and differential blood counts performed on a Hemavet HV950 (Drew Scientific Inc., Miami Lakes, FL).

Cohorts of additional mice were euthanized at indicated times after WBI, autopsied, and tissues were paraffin embedded and processed by the Translational Pathology Core at UCLA. Histopathological changes were examined by an expert animal pathologist (GL) on hematoxylin and eosin 0and picrosirius red collagen stained sections.

Immune subsets in bone marrow, blood, spleen and collagen/dispase-digested lung tissues were assessed after staining with antibody cocktails for the following markers: CD3, CD4, CD8, CD25, FoxP3, CD19, B220, CD11b, CD11c, Ly6G, Ly6C, F4/80, CD86, MHCII, lineage cocktail, c-kit, Sca-1, CD150, CD41 and CD48. Multi-color flow cytometry was performed on 100,000 collected events (LSRFortessa™; BD Biosciences, San Jose, CA) with FlowJo analysis (Ashland, OR).

The immune polarity of splenic lymphocytes was examined 48 h after *in vitro* stimulation with plate-bound anti-CD3 (BioCoat™; BD Biosciences) and soluble anti-CD28 (2 μg/ml) at 1×10^6 cells/well in X-VIVO™ 10 (Lonza™, Portsmouth, NH). Supernatants were stored at –80°C until cytokine antibody array assay (RayBiotech, Norcross, GA). Indirect enzyme-linked immuno-spot (ELISPOT) assay was also used for cells producing interferon-γ (IFN-γ) and IL-4 (BD Pharmingen™, Franklin Lakes, NJ) using MultiScreen®-HA plates (EMD Millipore, Billerica, MA) with cells reincubated for another 24 h and detection by biotinylated anti-mouse IFN-γ (BD Pharmingen), horseradish peroxidase avidin D (1:200 dilution; Vector® Laboratories, Burlingame, CA) and 0.4 mg/ml 3-amino-9-ethyla-carbazole as substrate (AEC; Sigma-Aldrich® LLC, St. Louis, MO). Spots were counted using the ImmunoSpot® Image Analyzer (Cellular Technology Ltd., Cleveland, OH).

Fecal Microbiome Analysis

Fecal pellets were collected from individual mice, into sterile 1.5-ml microcentrifuge tubes, snap frozen in liquid nitrogen and stored at –80°C. DNA was isolated using the QIAamp® DNA stool kit (QIAGEN®, Valencia, CA), according to the manufacturer's instructions. Bacterial DNA was amplified by a two-step PCR enrichment of the 16S rDNA (V4 region) encoding sequences with primers 515F and 806R modified by addition of barcodes for multiplexing. DNA was subsequently sequenced using the Personal Genome Machine (PGM™) System (Thermo Scientific™, Rockford, IL). Following quality filtering, the sequences were demultiplexed and trimmed before performing sequence alignments, identification of operational taxonomic units (OTU), clustering and phylogenetic analysis using QIIME open-source software (http://qiime.org).

Statistics

Kaplan-Meier plot with log-rank statistics was used to test for significance in survival differences. Multiple comparisons procedures were based on Sidak modified test. On data with insufficient homogeneity of variance, analyses of variance used the Brown-Forsythe test and the Kruskal-Wallis non-parametric test with less stringent assumptions for some cases. The differences in fecal microbiota between treatment groups were analyzed by non-parametric Kruskal-Wallis test (Dunn's multiple comparison test) and parametric *t* test with Welch correction. Significance was assessed at the 5% level using SPSS® version 20 software (Armonk, NY).

RESULTS

Changes in Patterns of Mortality during and after H-ARS Mitigation

Mortality data were compiled on groups of 613 male C3H mice with and without mitigator treatment that were derived from 16 independent experiments and followed for 660 days after 7.725 Gy WBI ($LD_{70/30}$). We have already reported on the efficacy of the six closely related NPS or NPSP compounds in mitigating H-ARS and that were used in this study (Supplementary Fig. S1; http://dx.doi.org/10.1667/RR15231.1.S1) (*33*). All six were tested using at least three different s.c. doses between 5 and 75 mg/kg, and up to five doses of 1, 2, 5, 25 and 75 mg/kg in the case of 1-[(4-nitrobenzene)sulfonyl]-4-phenylpiperazine (5355512), the lead compound. All groups had 8 mice. Not all drug doses were effective; to address this, we pooled groups of mice that did ($P < 0.05$) or did not ($P > 0.05$) have significantly increased survival over their respective diluent-only controls, which averaged at 33% survival. In general, active mitigators increased 30-day survival by more than 30%, and we ended up with three cohorts of ''active'' mitigators ($N = 197$ mice), ''less active'' mitigators ($N = 276$) and diluent-only controls ($N = 140$).

As expected, H-ARS lethality for all groups occurred between 10 and 30 days. For the ''active'' drug cohort, H-ARS survival at day 30 was 84.1% compared to 32.9% for the diluent cohort (Fig. 1A; $P < 0.0001$ Kaplan-Meier) and 59.4% for the ''less active'' cohort (not shown). As would be expected, ''active'' mitigators extended the median survival time (MST) during H-ARS from 17 days to 18.5 days ($P = 0.02$ log-rank test). This is consistent with the MST being inversely related to dose for any given ARS (*13, 14, 38*) and, since the probit dose-survival curves are parallel (*33*), mitigation of H-ARS can be regarded as quasi-dose-modifying.

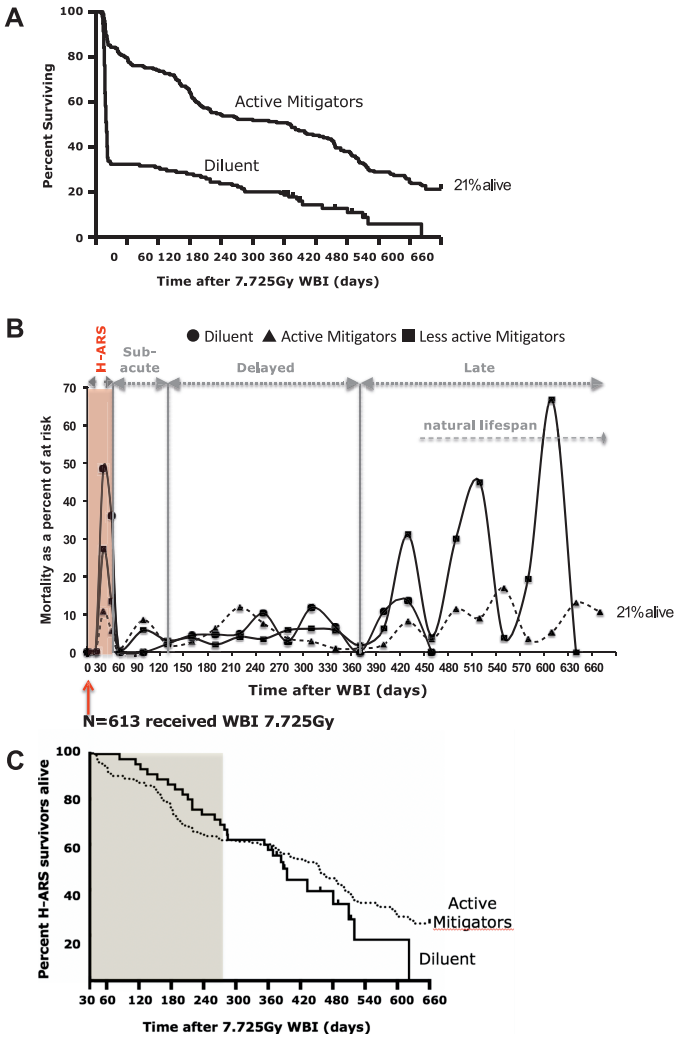

FIG. 1. Radiation mitigation of H-ARS alters mortality kinetics. Male C3H mice were whole-body irradiated with 7.725 Gy ($LD_{70/30}$), which induced H-ARS, and mice were followed for 660 days thereafter. Panel A: Kaplan-Meier plots show effective radiation mitigation of H-ARS with NPS or NPSP containing compounds that increased survival from 32.9% (diluent) to 84.1% ($P < 0.0001$) and resulted in 21% survival at day 660. Panel B: Waves of death recur in distinct phases that fit into an acute, subacute, delayed and late pattern. Mortality is shown as a percentage of animals at risk at any given point in time after statistically significant active mitigation, less active mitigation and diluent controls. Panel C: Kaplan-Meier plots for H-ARS 30-day survivors show temporary increased mortality during the subacute phase in the mitigated group but an overall slower rate of mortality and increased long-term survival in mitigated animals that survived H-ARS. Data are total remaining survivors starting at end of H-ARS, i.e., at 30 days after WBI at any given point in time thereafter.

Over the ensuing year, mortality rates ebbed and flowed relentlessly with a small number of deaths per month, but with some obvious nadirs at approximately 100, 250 and 340 days (Fig. 1B). A similar pattern of delayed mortality has been reported after WBI in mice receiving bone marrow rescue (*19*). For convenience, we consider there to be acute (<30 days), subacute (30–100 days), delayed (100–360 days) and late (>360 days) phases of mortality. It is important to distinguish the late phase, because it coincides with when C3H mice normally die from natural causes, which begins at approximately 500 days of age and results in a median lifespan of approximately 2 years of age (i.e., equivalent to 430 and 660 days after WBI, respectively); this is consistent with the published literature for this strain (*39*), which is known to be relatively short compared to other strains.

In the diluent controls, only one mouse died between 30 and 100 days (Fig. 1B). In contrast, there was 10% mortality in the active and less active mitigator cohorts combined (of 338 at risk; average survival 62 days; $P < 0.05$). In spite of this low-level subacute lethality and continuing attrition over the entire time period, some mice receiving active mitigation survived a normal life span, whereas none of the diluent controls did, and only a few in the less active mitigator cohort (Fig. 1B). This was because the rate of mortality was slower in those receiving active mitigation (Fig. 1C), being 3.9% per month compared to 6.1% per month for controls. As a result, at 1 year after WBI, survival was 50.3%, 38.8% and 11% in the active, less active and control cohorts, respectively, but only mice in the active mitigator cohort (21.3%) survived up to day 660 after WBI (N = 42). Although this is less than the 50% expected without WBI, clearly successful H-ARS mitigation translated into a long-term survival benefit.

Additional data were obtained in C57Bl/6 male mice (N = 136) with two of the NPSP mitigators: 1-[(4-nitrobenzene)sulfonyl]-4-phenylpiperazine (5355512) and 1-(3-chlorophenyl)-4-[(4-nitrobenzene)sulfonyl]piperazine (5346360) (*33*). This strain is more resistant to H-ARS and their $LD_{70/30}$ dose is higher at 8.509 Gy; otherwise the protocols were identical. As for C3H mice, the MST for H-ARS was slightly delayed by mitigation (21.25–22.9 days) and survival from H-ARS was increased from 29.2% to 73.2% (not shown). Subacute mortality patterns for C57BL/6 mice were very similar to C3H mice with no mice dying in the diluent cohort up to day 100 and 19% in the mitigated cohort (Supplementary Fig. S2; http://dx.doi.org/10.1667/RR15231.1.S1). Thereafter, the mortality patterns are less reliable because of small numbers of survivors, but at 1 year 43.8% were alive in the mitigated cohort compared to 20.8% of controls and only 2 control WBI C57BL/6 mice (8.3%) survived until day 430, compared to 34.8% in the mitigated cohort. The conclusions are therefore essentially the same in the two strains of mice, being that mitigation translates into long-term benefits for some, but not all, animals. We found no evidence of differences between female and male mice in their response to NPSP/NPS mitigators (*33*) or in their late mortalities, although the numbers were small (not shown).

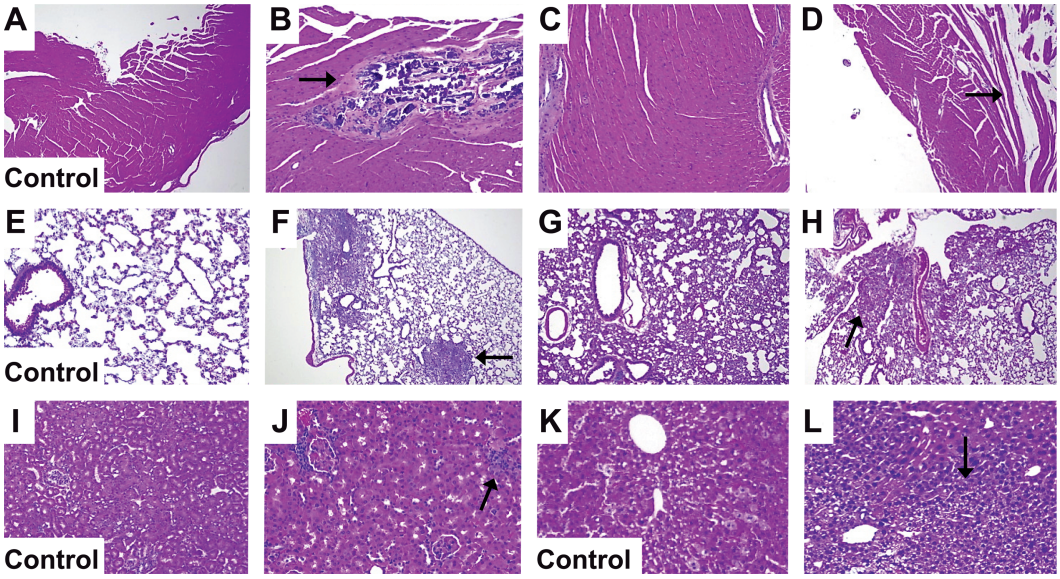

FIG. 2. Whole-body irradiation causes diverse, multi-organ pathologies that persist even after successful H-ARS mitigation. At 6 months after irradiation, heart (panels A–D), lung (panels E–H), kidney (panels I–J) and liver (panels K–L) were taken from cohorts of male C3H mice (most animals received 5 mg/kg 535512 H-ARS mitigation). Immunohistochemistry analysis on picrosirius red collagen-stained sections revealed occasional cardiac necrosis and mild fibrosis (panel B), mineralization of interventricular septa and the ventricular free walls (panel D), interstitial multifocal pneumonitis (panel G) and immune infiltrates with consolidation in lungs and some occasional focal scarring, and fibrosis (panel H), diffuse tubular degeneration sometimes with an inflammatory infiltrate with fibrosis and necrosis in kidney (panel J) and nodular hyperplasia with hepatic cell degeneration and disorganization in the liver (panel L). Control = aged-matched, nonirradiated mice (panels A, E, I and K).

Clinical and Pathological Changes after the H-ARS Period

Multiple, very complex histopathological changes have been reported in murine survivors of WBI (*8, 12, 15, 16, 18, 19, 40*), but their sporadic and diverse nature and low incidence over time makes it very difficult to attribute mortality to cause. Between 4 and 9 months after WBI, very close observation of cohorts of 100 mice showed that death was rapid, making necropsy practically impossible, with the only clinical symptoms being mild diarrhea that peaked transiently at 6–7 months (18%), occasional rectal prolapses (6%) and anemia (5%). Diarrhea was the only finding more frequent than death (8%) (Supplementary Table S1; http://dx.doi.org/10.1667/RR15231.1.S1). No tumors were found up to 9 months after WBI.

No diarrhea was detected in mice dying between 9 and 17 months after WBI, which encompasses the time when normal mice start to succumb to old age, but other clinical symptoms appeared, including progressive loss in body weight, a higher incidence of rectal prolapse (12%) and occasional tumors with incidence (10%) that was fairly low and late (Supplementary Table S1), perhaps diminished by death due to non-cancerous mortalities that precede cancer (*18*).

Because of the sporadic nature of clinical symptoms and deaths, cohorts of C3H mice with and without treatment with one highly effective NPSP mitigator (5355512; 5 mg/kg) were prospectively euthanized at 4 and 6 months after WBI to explore underlying pathologies in a defined setting. A spectrum of diverse lesions was observed in the lung, heart, liver and kidney of some, but not all animals (Fig. 2), as well as occasional splenic hyperplasia (not shown). Overall, approximately 60% of mice had some histopathological changes, with 33% having lesions involving more than one organ. Interestingly, lung lesions had a spectrum of histopathologies, including interstitial multifocal pneumonitis, mild interstitial immune infiltrates, perivascular lymphoid hyperplasia, occasional focal scarring and fibrosis (Fig. 2F–H). The diversity of the lesions was unexpected, since the C3H strain normally develops radiation pneumonitis after local thoracic irradiation, but very similar observations have been made late in Balb/c mice after WBI with bone marrow rescue (*19*). Liver lesions showed unusual mitotic cells and nodular hyperplasia with hepatic cell degeneration and disorganization (Fig. 2L). Changes in the kidney were generally diffuse tubular degeneration, sometimes with an inflammatory infiltrate (Fig. 2J). Cardiac lesions included mild fibrosis, mineralization of interventricular septa and the ventricular free walls and occasional necrosis (Fig. 2B–D). Only minimal changes were found in the gastrointestinal tract (not shown). The inter-mouse and intra-mouse variation greatly hindered more quantitative comparisons.

Immunological and Hematological Imbalances

The histopathology at 4 and 6 months clearly suggested chronic, but variable, immune or inflammatory cell

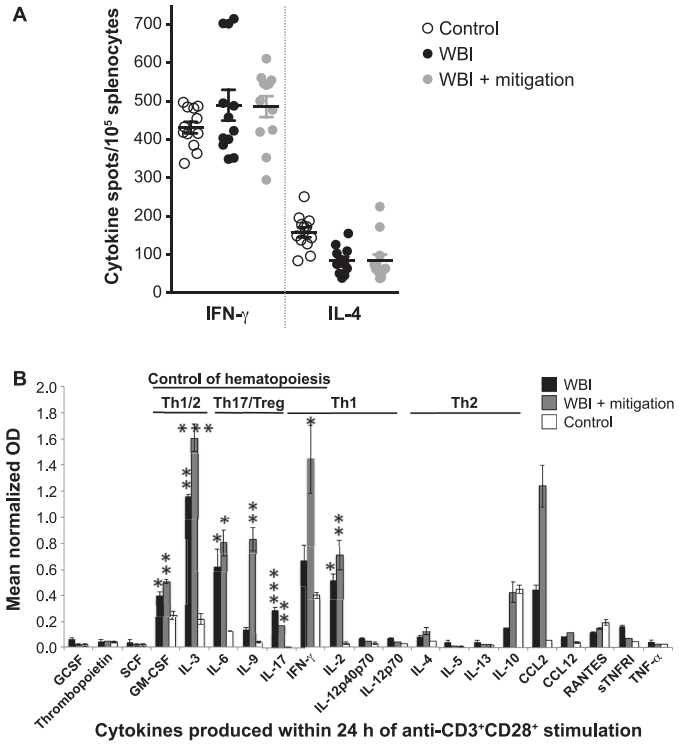

FIG. 3. C3H mice are naturally inclined towards a pro-inflammatory TH1 response, which is further polarized after irradiation. Splenocytes taken at 4 months after WBI with or without the NPSP mitigator 5355512 were *in vitro* stimulated with plate-bound anti-CD3 plus soluble anti-CD28 and assayed for T-cell polarity by IFN-γ and IL-4 ELISPOT after 48 h (panel A) and cytokine array after 24 h (panel B). Data are mean ± SEM of N = 4 mice/group with each N = 3 repeats (panel A) and N = 4 pooled spleen (panel B). $*P < 0.05$; $**P < 0.01$; $***P < 0.001$.

involvement in the delayed phase after WBI. A series of experiments were therefore initiated using the NPSP mitigator 535512 to assess changes in immune status at 4 months. Splenocytes were harvested from groups of WBI mice with and without mitigator treatment and activated *in vitro* with anti-CD3 plus anti-CD28 to determine immune T-cell polarity and function. ELISPOT assays revealed that, irrespective of mitigator treatment, WBI increased the number of cells producing the pro-inflammatory Th1-type cytokine IFN-γ, while Th2-type IL-4-producing cells decreased, though these changes did not reach statistical significance (Fig. 3A). The proclivity was however confirmed by ELISA of cytokines released into the supernatant from stimulated splenocytes (Fig. 3B), which showed markedly increased production of IFN-γ, IL-2, IL-6, IL-9 and IL-17, as well as the hematopoietic cytokines GM-CSF and IL-3, but not G-CSF, thrombopoietin, SCF or Th2-type cytokines. The increases were more marked in the mitigator group, which was not the case for ELISPOT (Fig. 3A). Since ELISA reports on released cytokines (at equal plated cell numbers) rather than the number of activated cells, the data suggest increased production of pro-inflammatory cytokines on a per cell basis after mitigation. Note that normal C3H mice tend to be biased towards the Th1 rather than Th2 axis ($P < 0.0001$), and WBI accentuates rather than changes this polarity.

Analysis of circulating blood cell counts at 4 months after WBI indicated full immunohematopoietic recovery in WBI mice with no effect of mitigation (Fig. 4A). However, compared to controls, white cell counts were higher and this appeared to be due to a lymphoid-to-myeloid shift. More detailed flow cytometric analysis of cellular phenotypes in the spleen showed a similar occasional shift towards myeloid lineages with increases in both classical macrophages and $Gr1^+$ myeloid cells (Fig. 4B). Since mitigation had no influence here, or in Fig. 4A, the WBI data were combined. The myeloid shift was accompanied by a decrease in $CD8^+$ T-cell populations and increases in $CD4^+$ T cells, in particular T-regulatory cells.

During these experiments, splenomegaly was noted in some mice, consistent with the splenic myeloid hyperplasia found by histopathology. The number of mice with splenomegaly varied by experiment, but with groups of 20 mice, the incidence of splenomegaly was 39% after WBI alone and 15% in mitigator-treated mice, contrasting with zero in controls. While these differences were not statistically significant, they alerted us to the possibility that systemic myeloid activation might explain some intra-experimental variability. Indeed, comparison of mice with and without splenomegaly (Fig. 4C) showed that splenomegaly accounted for almost all of the immunophenotypic changes. The myeloid shift was seen in all immune organs including bone marrow (not shown), which prompted us to examine its effect on hematopoietic stem cells. Indeed, mice with myeloid hyperplasia had increased $cKit^+Sca\text{-}1^+Lin^-$ (KSL) hematopoietic stem/progenitor bone marrow cells (HSPCs), but marked decreases in the long-term HSC $SLAM^+$ subset ($CD150^+CD48^-$), while both lineage-negative common lymphoid and myeloid progenitors were increased (Fig. 4D).

→

FIG. 4. Whole-body irradiation drives persistent immunohematopoietic imbalances with preferential myeloid skewing. Blood, spleen and bone marrow where taken from male C3H mice (8 per group) at 4 months after WBI (with or without the NPSP mitigator 5355512) and analyzed for their immune cell composition. Panel A: Differential blood counts read on Hemavet. Panel B: Immune cell profiles in the spleen assessed by flow cytometry. Panel C: Splenic immunophenotypes according to presence/absence of splenomegaly. Panel D: Hematopoietic stem/progenitor cell analysis by flow cytometry in the bone marrow. Data are mean ± SEM of N = 8.

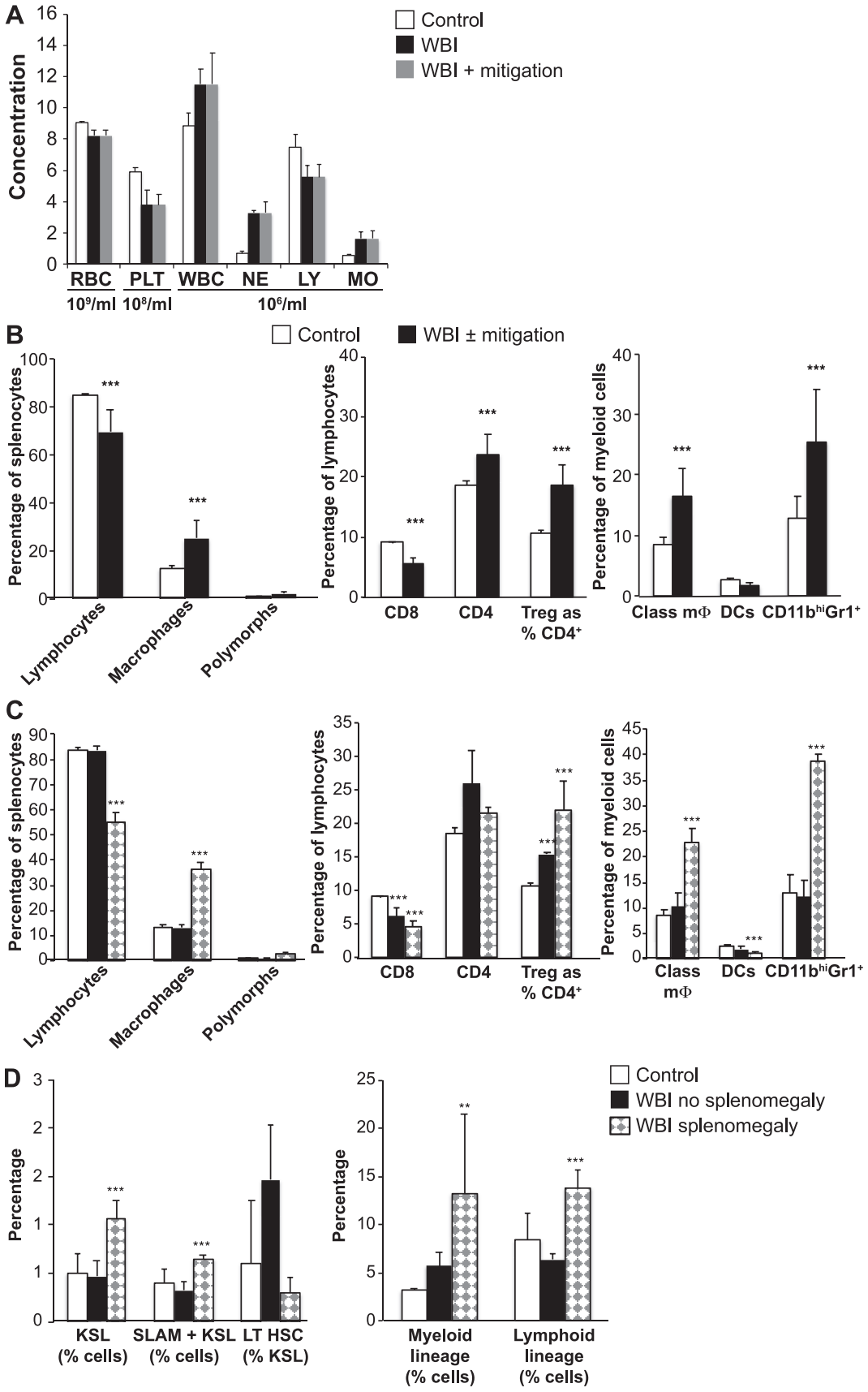
A
Concentration
Control
WBI
WBI + mitigation
RBC
PLT
WBC
NE
LY
MO
10⁹/ml
10⁸/ml
10⁶/ml
B
Control
WBI ± mitigation
Percentage of splenocytes
Lymphocytes
Macrophages
Polymorphs
Percentage of lymphocytes
CD8
CD4
Treg as % CD4⁺
Percentage of myeloid cells
Class mΦ
DCs
CD11b^hiGr1⁺
C
Percentage of splenocytes
Lymphocytes
Macrophages
Polymorphs
Percentage of lymphocytes
CD8
CD4
Treg as % CD4⁺
Percentage of myeloid cells
Class mΦ
DCs
CD11b^hiGr1⁺
D
Control
WBI no splenomegaly
WBI splenomegaly
Percentage
KSL (% cells)
SLAM + KSL (% cells)
LT HSC (% KSL)
Myeloid lineage (% cells)
Lymphoid lineage (% cells)

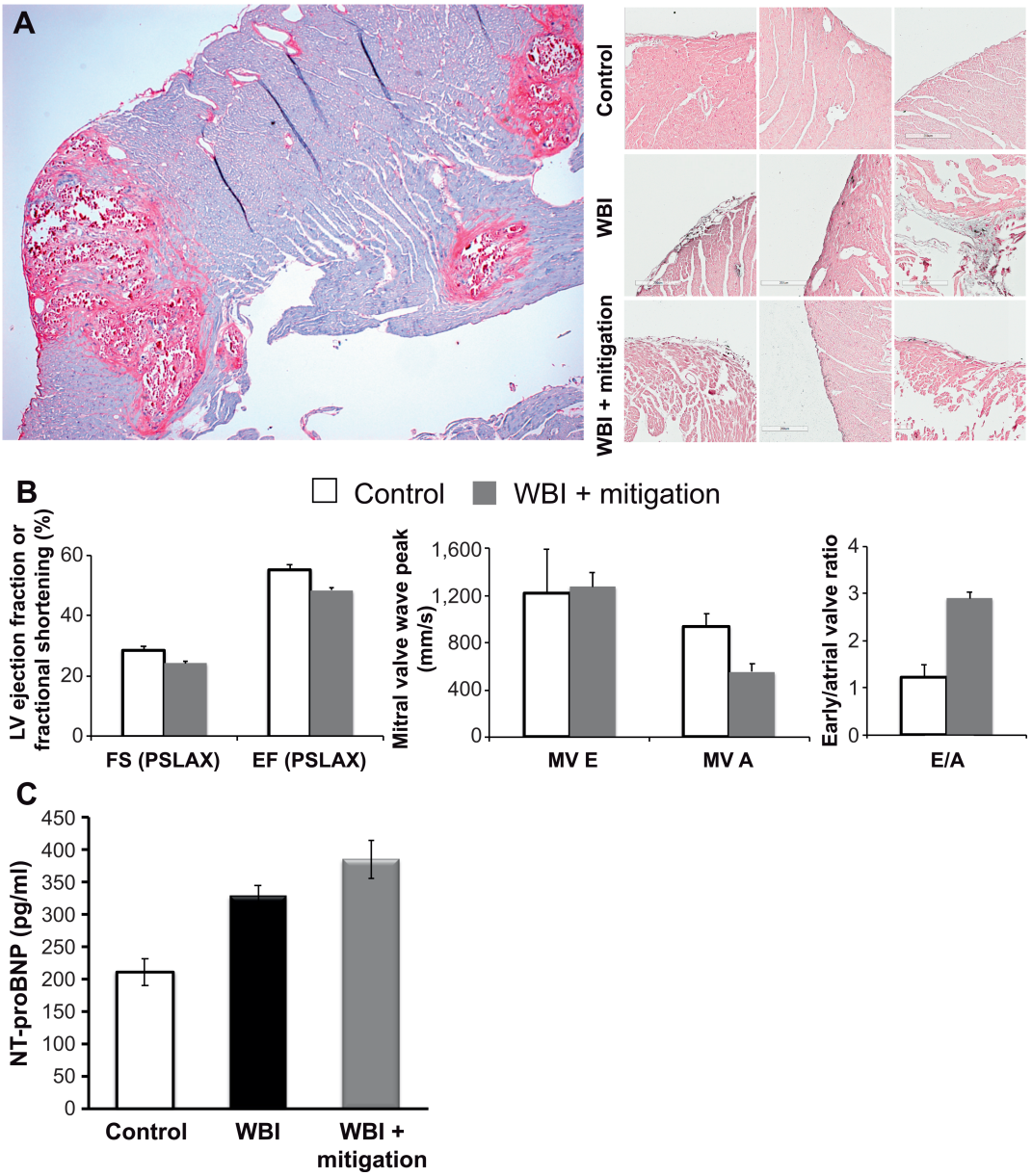

FIG. 5. Early mitigation of H-ARS does not prevent late radiation-induced cardiac damage and dysfunction. Panel A, left side: Picrosirius red collagen staining on heart sections at 4 months after WBI plus NPSP mitigator 5355512 (X50) showing cardiac fibrosis and necrosis. Panel A, right side: Heart sections stained for non-heme iron with enhanced Perl's Prussian blue stain. Panel B: Echocardiography on mice 100 days after WBI with mitigator 5355512 and aged-matched controls. Panel C: Circulating levels of NT-proB-type natriuretic peptide (NT-proBNP) measured by plasma ELISA at 6 months postirradiation. Data are mean of N = 6 ± SEM. FS = fractional shortening, EF = ejection fraction, MV = mitral valve.

Cardiac Complications

As mentioned earlier, cardiac inflammation and fibrosis was seen in some mice at 4 and 6 months after WBI, accompanied by accumulation of iron-coated macrophages in the pericardium (Fig. 5A). In our mice, the most obvious change detected by echocardiography was an increase in the early:atrial (E/A) wave ratio, which is generally indicative of hypertension, left ventricular hypertrophy or diastolic dysfunction (Fig. 5B). Plasma levels of NT-proB-type natriuretic peptide (NT-proBNP) were increased to a similar extent in both mitigated and control mice, indicating heart damage even at 6 months after WBI (Fig. 5C).

Changes in Intestinal Microbiota Composition

As mentioned in the subsection, Clinical and Pathological Changes after the H-ARS Period, mild diarrhea was found in 18% of mice 6–7 months after WBI (Supplementary Table S1; http://dx.doi.org/10.1667/RR15231.1.S1), and therefore we made preliminary efforts, using fecal samples from some of these mice, to investigate if the endogenous

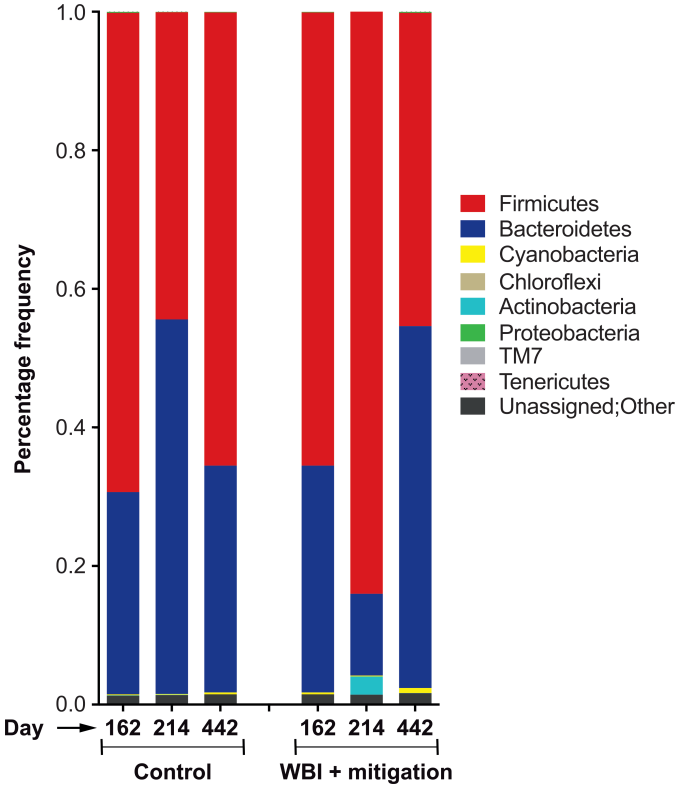

FIG. 6. Whole-body irradiation causes dynamic changes in the intestinal microbiome that relate to late morbidities even in the context of early H-ARS mitigation. Phylogenetic analysis of colonic microbiota in control and age-matched WBI mice treated with plerixafor plus NPSP 5355512. Fecal samples were collected from mice on day 162, 214 and 442 after irradiation (or control) and analyzed for the colonic microbiota by 16S rDNA enrichment and sequencing. Data are average relative abundance of each bacterial phylum. Control mice: N = 3 (day 162), N = 2 (day 214), N = 7 (day 442); WBI plus mitigator-treated mice: N = 3 (day 162), N = 3 (day 214), N = 2 (day 442).

intestinal microbiota was altered late after WBI. We collected fecal samples from individual mice sequentially on days 162, 214 and 442 after WBI plus mitigator treatment. The mitigator was 535512, as before, but in this case was administered with plerixafor (3.5 mg/kg, q.o.d. × 6); this treatment had no influence on mitigation or WBI-induced diarrhea. Phylogenetic analysis of 16S rDNA for OTU showed that the two major bacterial phyla in control nonirradiated mice were Bacteroidetes and Firmicutes, in agreement with previously published findings (*41*). We found no significant variation in fecal microbial composition as mice aged (Bacteroidetes, $P = 0.4886$; Firmicutes, $P = 0.4821$; N = 12) (Fig. 6). In contrast, on day 214 after WBI with mitigation, which was the peak time for diarrhea, the intestinal microbial community had altered significantly, most notably with a decrease in Bacteroidetes abundance ($P = 0.0315$; N = 8) (Fig. 6) and an increase in Firmicutes ($P = 0.0311$). Actinobacteria were relatively rare within the gut microbiota of nonirradiated control mice, independent of age, but fluctuated in WBI survivors, rising significantly on day 214 ($P = 0.0166$ compared to control).

DISCUSSION

Life shortening is a long-known consequence of WBI in experimental animals and humans, with cancer as the most frequently recognized cause. The gnotobiotic mice used in this study generally have a low cancer incidence, even in genetically susceptible strains, and overt infection after WBI is not seen until the mice are terminally ill. However, microbial products may still positively (*57*) or negatively (*41, 67*) influence long-term genotoxicity (*42*), inflammation (*43*) and stem cell niche function (*44, 45*), especially after WBI. In any event, we were unable to detect any cancers before mice entered old age, and even then only at approximately 10% incidence. Earlier non-cancerous deaths were the major cause of DEARE, which is in agreement with other published studies (*12*).

Ascribing cause to DEARE lethalities is difficult because of their low incidence rates even with high animal numbers. ARS can be ascribed to tissue-specific functional failure that occurs within a narrow dose-time window when small increases in dose rapidly increase lethality (*37*). We are therefore able to say with a high certainty that our ''active'' NSP mitigators increased the percentage of mice surviving H-ARS from 33% to 84%. This compares favorably with our experience with monovalent G-CSF (filgrastim 50–150 μg/kg, q.d. or q.o.d. × 9 or × 16) under identical conditions (85% 30-day survival; N = 40) or bivalent Fc-GCSF (73% 30-day survival, 50 μg/kg, q.o.d. × 9; N = 56).

Importantly, mortality rates for H-ARS-mitigated survivors were decreased compared to diluent controls and 25% lived for the expected median life span of normal mice of the same strain, while none of the unmitigated controls did, despite the higher mortality from 1–3 months after mitigated WBI. Our experience with long-term survival of H-ARS, resulting from mono- or di-valent G-CSF treatment, is numerically limited, but very few survived to a full life span, suggesting a need for additional mitigation for late effects after G-CSF. The cause of subacute deaths 1–3 months after WBI in the mitigated groups requires further investigation. Subacute failure in a specific hematopoietic compartment that is more radioresistant than that causing H-ARS, as has been noted in mini-pig H-ARS (*46*), seems unlikely, since the two systems are not actually comparable. Mortality in the subacute phase has been associated with erythroid failure by others (*40*), but we found no evidence of this by blood analyses (not shown).

DEARE lethality primarily involves multiple slowly-proliferating organ systems, such as the lung, heart, kidney and liver (*47*), that respond late to radiation. The diarrhea that was observed at 6 months after WBI may be an exception, as the epithelium proliferates rapidly; however, damage in this case may have been consequential to acute damage (although histopathological evidence was lacking), or due to changes in the microbiome. Our observation that the gut microbiome alters in favor of Firmicutes and Actinobacteria and away from Bacteroidetes at the time of

peak diarrhea is not too dissimilar to the microbiome shifts that have been observed in patients with intestinal and oral cancer during radiotherapy (*48, 49*) and may serve as a DEARE biomarker (*50*). Such dynamic changes at the host-microbiome interface may ultimately affect the manifestation of tissue toxicity as seen in mucositis (*51*), chemotherapy-induced gastrointestinal toxicity (*52*) and gut dysbiosis (*41*) and may, at least in part, account for the sporadic nature of DEARE, a variability that is perhaps its most confusing aspect.

Pulmonary damage may not be surprising as the lung is generally accepted as the dose-limiting tissue after WBI (*19*). However, models of local radiation-induced lung damage use higher doses and show a limited histopathology, unlike the great variability that we and others see after WBI (*19*). In fact, multiple organs show a spectrum of changes that vary among different animals after WBI. The heart damage we have seen in our mice also develops in humans (*53*) and in NHPs after WBI (*30*). Indeed, radiation-induced cardiac disease at relatively low doses is of growing interest as a potential clinical complication (*54*). The most common radiation change is left ventricular dysfunction, as shown here, but cardiovascular radiation disease can be more complex. Radiotherapy involving the mediastinum causes linear increases in the rates of myocardial infarction, coronary revascularization or death from ischemic heart disease by 7.4% per Gy within a few years (*53*), with pathologies that can include microvascular loss or arterial lesions, fibrosis of the pericardium and myocardium and pericardial adhesions. In the studies of C57BL/6 mice, using heart-only irradiation, Seemann *et al.* (*55*) noted modest decreases in end diastolic and systolic volumes and increased ejection fraction 20 and 40 weeks after 2, 8 and 16 Gy irradiation, with inflammatory changes and microvascular loss at 20 weeks after 8 Gy, although these did not deteriorate despite progressive structural and microvascular damage. The same has been observed after non-fatal WBI (*47*). The extent to which cardiac damage contributes to lethality, with or without mitigation, is therefore still uncertain.

The histopathology after WBI seen in this study is similar to reports after WBI with bone marrow rescue (*19*) or after partial-body shielding (*57*). The oscillating waves of premature mortalities that we observed can also occur after local irradiation, for example of the thorax (*56*). These cyclical patterns are reminiscent of the waves of inflammatory cytokines we have seen after irradiation of various tissues (*57–60*). The general paradigm that emerges is one where ARS survivors come out of a limited dose–time mortality window only to experience recurring and persistent crises, each with an elevated probability of premature death. The simplest hypothesis may be that the driver of these responses is radiation-induced cell death associated with turnover of lethally damaged cells or senescence occurring in different organs at different times, leading to loss of stem/progenitor cells. However, a more comprehensive hypothesis would be that recognition of micronuclei (*61, 62*), microbes or damage-associated immune responses (*63, 64*) trigger further late damage expression through generating chronic inflammation.

This raises the important question of whether any mitigator is truly ''dose modifying'' for all tissues and how it affects these complex processes. Our lead compound mitigates not only H-ARS, but also intestinal ARS and radiation pneumonitis and lung fibrosis (*33*), in keeping with a systemic influence; and our studies point to myeloid hyperplasia and associated functional changes in the immunohematopoietic system (*33*) as playing a major role in DEARE, and in its individual variability. Part of the response to radiation involves rapid mobilization of bone marrow-derived myeloid cells that act as first responders to danger (*13, 33*). This triggers downstream common myeloid progenitors to replenish cells of the myeloid and erythroid system that ''die in action'' (*62*), that decrease GI-ARS (*14, 65, 66*) by forming stem cell niches (*61*) and that heal radiation-induced wound-healing defects (*67*). Perhaps chronic late life-shortening is the price that must be paid for acute life-saving myelopoiesis.

We hypothesize that this myeloid skewing persists in some mice, as is seen in splenomegaly and increased myeloid cell representation in various organs, and this promotes DEARE through the drivers mentioned above. Our mitigators appear to limit myeloid skewing, although further work is needed to confirm this. Similar myeloid skewing in humans and mice has been associated with aging, chronic inflammation and autoimmunity (*44, 68, 69*), indicating common immune-based mechanisms. The importance of the myeloid system is further appreciated by the fact that myeloid skewing comes at the expense not only of $CD8^+$ lymphocytes but also the most primitive long-term repopulating KSL cells, shifting the hematopoietic balance towards more differentiated progenitors (*45*).

Perhaps the most striking observation of this study is that animals of the same age, strain and gender receiving the same dose of WBI can have very different long-term outcomes. We hypothesize that this is due to the stochastic nature of chronic inflammatory myeloid skewing that has systemic effects, including imbalance of homeostasis in the immunohematopoietic system, with inflammatory and metabolic consequences. In any event, we hypothesize that the shifts in myeloid cells and in the microbiome might be good biomarkers of DEARE and targets for further therapeutic intervention. This concept of the importance of systemic and persistent activation of cells after WBI is not new. Mole reached a similar conclusion in 1953, suggesting that WBI interferes with the interdependence between cells and tissues to cause abscopal effects, resulting in damage beyond what was expected (*70*). This interdependence may be affected by radiation damage to tissues additional to those investigated here, e.g., endocrine systems; however, the myeloid activation still appears to be a driver and obvious and ever-present component of DEARE.

SUPPLEMENTARY INFORMATION

Table S1. Frequency of common morbidities and mortalities in a cohort of 100 male C3H mice up to 17 months after whole-body irradiation.

Fig. S1. Chemical structures of the six related 4-(nitrophenylsulfonyl)piperazines (NPSP) and 4-nitrophenyl-sulfonamides (NPS) compounds that were tested for their ability to mitigate H-ARS and extend long-term survival in whole-body irradiated mice. A total of 613 male C3H mice in 61 experimental groups were treated in this study.

Fig. S2. Successful mitigation of H-ARS in irradiated C57Bl/6 mice also changes mortality kinetics long-term. An increase in MST and survival during H-ARS are the hallmark signs for successful H-ARS mitigation, as is improved long-term survival. Whole-body irradiation of male C57Bl/6 mice (N = 136) with 8.509 Gy ($LD_{70/30}$) causes H-ARS and rapid death within the 30-day window. Effective radiation mitigation using the NPS-containing compounds 5355512 and 5346360 given for the first 5 days postirradiation (N = 112) allowed survival to increase from 29.2% (N = 7, diluent) to 73.2% (N = 82, mitigator) during the acute phase and from 8.3% (N = 2, diluent) to 34.8% (N = 39, mitigator) overall (430 days).

ACKNOWLEDGMENT

This work was supported by a National Institutes of Health (award no. U19 AI067769) to the UCLA Center for Medical Countermeasures against Radiation.

Received: September 7, 2018; accepted: January 22, 2019; published online: February 7, 2019

REFERENCES

1. Epperly MW, Sacher JR, Krainz T, Zhang X, Wipf P, Liang M, et al. Effectiveness of analogs of the GS-nitroxide, JP4-039, as total body irradiation mitigators. In Vivo 2017; 31:39–43.
2. Burdelya LG, Krivokrysenko VI, Tallant TC, Strom E, Gleiberman AS, Gupta D, et al. An agonist of toll-like receptor 5 has radioprotective activity in mouse and primate models. Science 2008; 320:226–30.
3. Shakhov AN, Singh VK, Bone F, Cheney A, Kononov Y, Krasnov P, et al. Prevention and mitigation of acute radiation syndrome in mice by synthetic lipopeptide agonists of Toll-like receptor 2 (TLR2). PLoS One 2012; 7:e33044.
4. Katoch O, Khan GA, Dwarakanath BS, Agrawala PK. Mitigation of hematopoietic radiation injury by diallyl sulphide. J Environ Pathol Toxicol Oncol 2012; 31:357–65.
5. Casey-Sawicki K, Zhang M, Kim S, Zhang A, Zhang SB, Zhang Z, et al. A basic fibroblast growth factor analog for protection and mitigation against acute radiation syndromes. Health Phys 2014; 106:704–12.
6. Himburg HA, Yan X, Doan P, Quarmyne M, Micewicz E, McBride WH, et al. Therapeutic hematopoietic regeneration via pleiotropin-mediated activation of Ras. J Clin Invest 2014; 124:4753–8.
7. Kim K, Pollard JM, Norris AJ, McDonald JT, Sun Y, Micewicz E, et al. High-throughput screening identifies two classes of antibiotics as radioprotectors: tetracyclines and fluoroquinolones. Clin Cancer Res 2009; 15:7238–45.
8. Mole RH. Life shortening by multiple doses of irradiation. Gerontologia 1959; 3:159–60.
9. Kallman RF, Kohn HI. Life shortening by whole- and partial-body X-irradiation in mice. Science 1958; 128:301–2.
10. Yuhas JM. The dose response curve for radiation-induced life shortening. J Gerontol 1969; 24:451–6.
11. Paunesku D, Paunesku T, Wahl A, Kataoka Y, Murley J, Grdina DJ, et al. Incidence of tissue toxicities in gamma ray and fission neutron-exposed mice treated with Amifostine. Int J Radiat Biol 2008; 84:623–34.
12. Cosgrove GE, Upton AC, Congdon CC, Doherty DG, Christenberry KW, Gosslee DG. Late somatic effects of X-radiation in mice treated with aet and isologous bone marrow. Radiat Res 1964; 21:550–74.
13. Bond VP, Fludner TM, Archambeau JO. Mammalian radiation lethality. New York: Academic Press; 1965.
14. Mason KA, Withers HR, McBride WH, Davis CA, Smathers JB. Comparison of the gastrointestinal syndrome after total-body or total abdominal irradiation. Radiat Res 1989; 117:480–8.
15. Lindop PJ, Rotblat J. Shortening of life and causes of death in mice exposed to a single whole-body dose of radiation. Nature 1961; 189:645–8.
16. Lindop PJ, Rotblat J. The age factor in the susceptibility of man and animals to radiation. I. The age factor in radiation sensitivity in mice. Br J Radiol 1962; 35:23–31.
17. Williams JP, Brown SL, Georges GE, Hauer-Jensen M, Hill RP, Huser AK, et al. Animal models for medical countermeasures to radiation exposure. Radiat Res 2010; 173:557–78.
18. Anderson RE, Scaletti JV, Howarth JL. Radiation-induced life shortening in germfree mice. Exp Gerontol 1972; 7:289–301.
19. Travis EL, Peters LJ, McNeill J, Thames HD Jr., Karolis C. Effect of dose-rate on total body irradiation: lethality and pathologic findings. Radiother Oncol 1985; 4:341–51.
20. Yamada M, Wong FL, Fujiwara S, Akahoshi M, Suzuki G. Noncancer disease incidence in atomic bomb survivors, 1958–1998. Radiat Res 2004; 161:622–32.
21. Stewart AM, Kneale GW. A-bomb radiation and evidence of late effects other than cancer. Health Phys 1990; 58:729–35.
22. Nakachi K, Hayashi T, Hamatani K, Eguchi H, Kusunoki Y. Sixty years of follow-up of Hiroshima and Nagasaki survivors: current progress in molecular epidemiology studies. Mutat Res 2008; 659:109–17.
23. Kusunoki Y, Yamaoka M, Kubo Y, Hayashi T, Kasagi F, Douple EB, et al. T-cell immunosenescence and inflammatory response in atomic bomb survivors. Radiat Res 2010; 174:870–6.
24. Hsu W-L, Tatsukawa Y, Neriishi K, Yamada M, Cologne J, Fiujiwara S. Longitudinal trends of total white blood cell and differentialwhite blood cell counts of atomic bomb survivors. J Radiat Res 2010; 51:431–9.
25. Neriishi K, Nakashima E, Delongchamp RR. Persistent subclinical inflammation among A-bomb survivors. Int J Radiat Biol 2001; 77:475–82.
26. Endo A, Yamaguchi Y. Analysis of dose distribution for heavily exposed workers in the first criticality accident in Japan. Radiat Res 2003; 159:535–42.
27. Hirama T, Akashi M. Multi-organ involvement in the patient who survived the Tokai-mura criticality accident. BJR Suppl 2005; 27:17–20.
28. Krestinina LY, Epifanova S, Silkin S, Mikryukova L, Degteva M, Shagina N, et al. Chronic low-dose exposure in the Techa River Cohort: risk of mortality from circulatory diseases. Radiat Environ Biophys 2013; 52:47–57.
29. Kavanagh K, Dendinger MD, Davis AT, Register TC, DeBo R, Dugan G, et al. Type 2 diabetes is a delayed late effect of whole-body irradiation in nonhuman primates. Radiat Res 2015; 183:398–406.
30. DeBo RJ, Lees CJ, Dugan GO, Caudell DL, Michalson KT, Hanbury DB, et al. Late effects of total-body gamma irradiation on cardiac structure and function in male rhesus macaques. Radiat Res 2016; 186:55–64.

31. Storer JB. Chemical protection of the mouse against radiation-induced life shortening. Radiat Res 1971; 47:537–47.

32. Loghmani F, Mohammed KA, Nasreen N, Van Horn RD, Hardwick JA, Sanders KL, et al. Inflammatory cytokines mediate C-C (monocyte chemotactic protein 1) and C-X-C (interleukin 8) chemokine expression in human pleural fibroblasts. Inflammation 2002; 26:73–82.

33. Micewicz ED, Kim K, Iwamoto KS, Ratikan JA, Cheng G, Boxx GM, et al. 4-(Nitrophenylsulfonyl)piperazines mitigate radiation damage to multiple tissues. PLoS One 2017; 12:e0181577.

34. Goloshchapov PV, Vorob'eva MI. [Shortening of the life span in an experiment with chronic external gamma-irradiation. In defense of the aging hypothesis]. Radiobiologiia 1987; 27:501–4.

35. Bertell R. X-ray exposure and premature aging. J Surg Oncol 1977; 9:379–91.

36. Armenian SH, Horak D, Scott JM, Mills G, Siyahian A, Berano Teh J, et al. Cardiovascular function in long-term hematopoietic cell transplantation survivors. Biol Blood Marrow Transplant 2017; 23:700–5.

37. Williams JP, McBride WH. After the bomb drops: a new look at radiation-induced multiple organ dysfunction syndrome (MODS). Int J Radiat Biol 2011; 87:851–68.

38. Cronkite EP, Brecher G. The protective effect of granulocytes in radiation injury. Ann N Y Acad Sci 1955; 59:815–33.

39. Yuan R, Tsaih SW, Petkova SB, Marin de Evsikova C, Xing S, Marion MA, et al. Aging in inbred strains of mice: study design and interim report on median lifespans and circulating IGF1 levels. Aging Cell 2009; 8:277–87.

40. Sacher GA, Grahn D. Survival of mice under duration-of-life exposure to gamma rays. I. the dosage-survival relation and the lethality function. J Natl Cancer Inst 1964; 32:277–321.

41. Deriu E, Boxx GM, He X, Pan C, Benavidez SD, Cen L, et al. Influenza virus affects intestinal microbiota and secondary salmonella infection in the gut through type I interferons. PLoS Pathog 2016; 12:e1005572.

42. Udroiu I, Antoccia A, Sgura A. Long-term genotoxic effects in the hematopoietic system of prenatally X-irradiated mice. Int J Radiat Biol. 2017; 93:261–9.

43. Westbrook AM, Wei B, Hacke K, Xia M, Braun J, Schiestl RH. The role of tumour necrosis factor-alpha and tumour necrosis factor receptor signalling in inflammation-associated systemic genotoxicity. Mutagenesis 2012; 27:77–86.

44. Shao L, Feng W, Li H, Gardner D, Luo Y, Wang Y, et al. Total body irradiation causes long-term mouse BM injury via induction of HSC premature senescence in an Ink4a- and Arf-independent manner. Blood 2014; 123:3105–15.

45. McCabe A, MacNamara KC. Macrophages: Key regulators of steady-state and demand-adapted hematopoiesis. Exp Hematol 2016; 44:213–22.

46. Moroni M, Elliott TB, Deutz NE, Olsen CH, Owens R, Christensen C, et al. Accelerated hematopoietic syndrome after radiation doses bridging hematopoietic (H-ARS) and gastrointestinal (GI-ARS) acute radiation syndrome: early hematological changes and systemic inflammatory response syndrome in minipig. Int J Radiat Biol 2014; 90:363–72.

47. Carnes BA, Gavrilova N, Grahn D. Pathology effects at radiation doses below those causing increased mortality. Radiat Res 2002; 158:187–94.

48. Nam YD, Kim HJ, Seo JG, Kang SW, Bae JW. Impact of pelvic radiotherapy on gut microbiota of gynecological cancer patients revealed by massive pyrosequencing. PLoS One 2013; 8:e82659.

49. Zhu XX, Yang XJ, Chao YL, Zheng HM, Sheng HF, Liu HY, et al. The potential effect of oral microbiota in the prediction of mucositis during radiotherapy for nasopharyngeal carcinoma. EBioMedicine. 2017; 18:23–31.

50. Lam V, Moulder JE, Salzman NH, Dubinsky EA, Andersen GL, Baker JE. Intestinal microbiota as novel biomarkers of prior radiation exposure. Radiat Res 2012; 177:573–83.

51. Touchefeu Y, Montassier E, Nieman K, Gastinne T, Potel G, Bruley des Varannes S, et al. Systematic review: the role of the gut microbiota in chemotherapy- or radiation-induced gastrointestinal mucositis - current evidence and potential clinical applications. Aliment Pharmacol Ther 2014; 40:409–21.

52. Forsgard RA, Marrachelli VG, Korpela K, Frias R, Collado MC, Korpela R, et al. Chemotherapy-induced gastrointestinal toxicity is associated with changes in serum and urine metabolome and fecal microbiota in male Sprague-Dawley rats. Cancer Chemother Pharmacol 2017; 80:317–32.

53. Darby SC, Cutter DJ, Boerma M, Constine LS, Fajardo LF, Kodama K, et al. Radiation-related heart disease: current knowledge and future prospects. Int J Radiat Oncol Biol Phys 2010; 76:656–65.

54. Baker JE, Moulder JE, Hopewell JW. Radiation as a risk factor for cardiovascular disease. Antioxid Redox Signal 2011; 15:1945–56.

55. Seemann I, Gabriels K, Visser NL, Hoving S, te Poele JA, Pol JF, et al. Irradiation induced modest changes in murine cardiac function despite progressive structural damage to the myocardium and microvasculature. Radiother Oncol 2012; 103:143–50.

56. Tucker SL, Travis EL. Time course for the hazard of radiation-induced pneumonitis death in mice. Int J Radiat Biol 1992; 62:627–39.

57. Schaue D, Kachikwu EL, McBride WH. Cytokines in radiobiological responses: a review. Radiat Res 2012; 178:505–23.

58. Schaue D, Micewicz ED, Ratikan JA, Xie MW, Cheng G, McBride WH. Radiation and inflammation. Semin Radiat Oncol 2015; 25:4–10.

59. McBride WH, Chiang CS, Olson JL, Wang CC, Hong JH, Pajonk F, et al. A sense of danger from radiation. Radiat Res 2004; 162:1–19.

60. Chiang CS, Hong JH, Stalder A, Sun JR, Withers HR, McBride WH. Delayed molecular responses to brain irradiation. Int J Radiat Biol 1997; 72:45–53.

61. Rodier F, Munoz DP, Teachenor R, Chu V, Le O, Bhaumik D, et al. DNA-SCARS: distinct nuclear structures that sustain damage-induced senescence growth arrest and inflammatory cytokine secretion. J Cell Sci 2011; 124 (Pt 1):68–81.

62. Beach TA, Johnston CJ, Groves AM, Williams JP, Finkelstein JN. Radiation induced pulmonary fibrosis as a model of progressive fibrosis: Contributions of DNA damage, inflammatory response and cellular senescence genes. Exp Lung Res 2017; 43:134–49.

63. Harding SM, Benci JL, Irianto J, Discher DE, Minn AJ, Greenberg RA. Mitotic progression following DNA damage enables pattern recognition within micronuclei. Nature 2017; 548:466–70.

64. Vanpouille-Box C, Formenti SC, Demaria S. TREX1 dictates the immune fate of irradiated cancer cells. Oncoimmunology 2017; 6:e1339857.

65. Saha S, Aranda E, Hayakawa Y, Bhanja P, Atay S, Brodin NP, et al. Macrophage-derived extracellular vesicle-packaged WNTs rescue intestinal stem cells and enhance survival after radiation injury. Nat Commun 2016; 7:13096.

66. Terry NH, Travis EL. The influence of bone marrow depletion on intestinal radiation damage. Int J Radiat Oncol Biol Phys 1989; 17:569–73.

67. Vegesna V, Withers HR, Holly FE, McBride WH. The effect of local and systemic irradiation on impairment of wound healing in mice. Radiat Res 1993; 135:431–3.

68. Dawar S, Shahrin NH, Sladojevic N, D'Andrea RJ, Dorstyn L, Hiwase DK, et al. Impaired haematopoietic stem cell differentiation and enhanced skewing towards myeloid progenitors in aged caspase-2-deficient mice. Cell Death Dis 2016; 7:e2509.

69. Oduro KA Jr., Liu F, Tan Q, Kim CK, Lubman O, Fremont D, et al. Myeloid skewing in murine autoimmune arthritis occurs in hematopoietic stem and primitive progenitor cells. Blood 2012; 120:2203–13.

70. Mole RH. Whole body irradiation; radiobiology or medicine? Br J Radiol 1953; 26:234–41.